J Membrane Biol (2014) 247:971–980
DOI 10.1007/s00232-014-9701-9

Nanoparticle Surface-Enhanced Raman Scattering of Bacteriorhodopsin Stabilized by Amphipol A8-35

V. Polovinkin · T. Balandin · O. Volkov · E. Round · V. Borshchevskiy · P. Utrobin · D. von Stetten · A. Royant · D. Willbold · G. Arzumanyan · V. Chupin · J.-L. Popot · V. Gordeliy

Received: 26 February 2014 / Accepted: 16 June 2014 / Published online: 6 September 2014

Abstract Surface-enhanced Raman spectroscopy (SERS) has developed dramatically since its discovery in the 1970s, because of its power as an analytical tool for selective sensing of molecules adsorbed onto noble metal nanoparticles (NPs) and nanostructures, including at the single-molecule (SM) level. Despite the high importance of membrane proteins (MPs), SERS application to MPs has not really been studied, due to the great handling difficulties resulting from the amphiphilic nature of MPs. The ability of amphipols (APols) to trap MPs and keep them soluble, stable, and functional opens up onto highly interesting applications for SERS studies, possibly at the SM level. This seems to be feasible since single APol-trapped MPs can fit into gaps between noble metal NPs, or in other gap-containing SERS substrates, whereby the enhancement of Raman scattering signal may be sufficient for SM sensitivity. The goal of the present study is to give a proof of concept of SERS with APol-stabilized MPs, using bacteriorhodopsin (BR) as a model. BR trapped by APol A8-35 remains functional even after partial drying at a low humidity. A dried mixture of silver Lee–Meisel colloid NPs and BR/A8-35 complexes give rise to SERS with an average enhancement factor in excess of 10^2. SERS spectra resemble non-SERS spectra of a dried sample of BR/APol complexes.

Electronic supplementary material The online version of this article (doi:10.1007/s00232-014-9701-9) contains supplementary material, which is available to authorized users.

V. Polovinkin · P. Utrobin · A. Royant · V. Gordeliy (✉)
Univ. Grenoble Alpes, IBS, 38044 Grenoble, France
e-mail: valentin.gordeliy@ibs.fr

V. Polovinkin · P. Utrobin · A. Royant · V. Gordeliy
CNRS, IBS, 38044 Grenoble, France

V. Polovinkin · P. Utrobin · A. Royant · V. Gordeliy
CEA, IBS, 38044 Grenoble, France

V. Polovinkin · V. Borshchevskiy · V. Chupin · V. Gordeliy
Laboratory for Advanced Studies of Membrane Proteins, Moscow Institute of Physics and Technology, 141700 Dolgoprudny, Moscow Region, Russia

T. Balandin · O. Volkov · E. Round · V. Borshchevskiy · D. Willbold · V. Gordeliy
Institute of Complex Systems (ICS), ICS-6: Structural Biochemistry, Research Centre Juelich, 52425 Juelich, Germany

O. Volkov
Institute of Crystallography, University of Aachen (Rheinisch-Westfälische Technische Hochschule), 52056 Aachen, Germany

D. von Stetten · A. Royant
European Synchrotron Radiation Facility, 38027 Grenoble, France

D. Willbold
Institut für Physikalische Biologie, Heinrich-Heine-Universität Düsseldorf, 40225 Düsseldorf, Germany

G. Arzumanyan
Multi Access Centre "Nanobiophotonics", Joint Institute for Nuclear Research, 141980 Dubna, Moscow Region, Russia

J.-L. Popot
Laboratoire de Physico-Chimie Moléculaire des Membranes Biologiques, UMR 7099, Institut de Biologie Physico-Chimique (CNRS FRC 550), Centre National de la Recherche Scientifique and Université Paris-7, 13 rue Pierre et Marie Curie, 75005 Paris, France

Keywords Amphipol · Membrane protein · Bacteriorhodopsin · SERS spectroscopy · Silver nanoparticles

Introduction

It has long been recognized that Raman scattering (RS) is one of the most informative spectroscopic techniques (Carey 1982) to study biological macromolecules. This vibrational spectroscopy provides information about conformational states of the analytes and their intra- and intermolecular interactions. For example, the changes in molecular conformation that characterize many molecular biological phenomena can produce large changes in Raman band positions (Carey 1982; Peticolas 1995; Benevides et al. 2004). By monitoring these frequency shifts, one can analyze secondary structures and detect ligand-induced conformational changes of biomolecules.

Despite the considerable advantages of RS for biological studies, the very small cross section of biological molecules ($\sim 10^{-30}$ to 10^{-24} cm^2 per molecule) limits applications of this vibrational spectroscopy. In particular RS does not possess single-molecule (SM) sensitivity (Kneipp et al. 2006; Le Ru and Etchegoin 2012). To compare, fluorescence cross sections are $\sim 10^{-16}$ cm^2 per molecule.

Discovered in 1974 (Fleischmann et al. 1974; Jeanmaire and Van Duyne 1977; Albrecht and Creighton 1977), surface-enhanced Raman scattering (SERS) provides greater sensitivity than conventional RS (Moskovits 1985; Otto 1984). Because it provides Raman enhancement factors (EFs) in the range of 10^4–10^{11}, SERS is becoming a powerful technique for probing biological molecules adsorbed onto noble metal nanostructured surfaces (Kneipp et al. 2006; Le Ru and Etchegoin 2012). The enhancement mechanism originates in part from the large local electromagnetic fields caused by resonant surface plasmons that can be optically excited at certain wavelengths for noble metal nanoparticles (NPs) of different shapes, compact assemblies of NPs, or noble metal nanostructures. In addition, metal nanostructures and analytes can form charge-transfer complexes, providing further enhancement of SERS (Otto 1984; Stiles et al. 2008).

The enhancement of Raman signals can be up to $\sim 10^9$ to 10^{11} if the analyte lies in so-called "hot spots," which are usually highly localized regions (Le Ru et al. 2006a), typically gaps between silver and gold nanostructures. The "hot spot" enhancement can then be large enough to allow single-molecule Raman spectroscopy (Nie and Emory 1997; Kneipp et al. 1997; Xu et al. 2000; Jiang et al. 2003; Futamata et al. 2005; Futamata 2006; Le Ru et al. 2006b).

Considerable efforts have been made to exploit the non-destructive nature of Raman spectroscopy, along with its high information content, for spectroscopic studies of single biomolecules, and as a basis of supersensitive biosensors. There are good examples of using SERS for studying and sensing proteins (Chumanov et al. 1990; Nabiev et al. 1990; Drachev et al. 2005). For instance, SERS can distinguish between two insulin isomers, human insulin and its analogue insulin lispro (Drachev et al. 2004). SM SERS of several water-soluble proteins has also been achieved (Xu et al. 1999; Habuchi et al. 2003; Delfino et al. 2006). There is, however, little information about applying SERS to membrane proteins (MPs) (Nabiev et al. 1990; Hrabakova et al. 2006; Naumann et al. 2006; Deckert-Gaudig et al. 2012), and no examples of successful MP SM SERS studies. Yet, MPs are among the most important biological targets: they comprise about one-third of the human genome (Krogh et al. 2001), perform the main functions of biological membranes, and are of great interest to the pharmaceutical industry, around 60 % of all current drugs targeting MPs (Overington et al. 2006).

MPs are difficult to study because of their amphiphilic nature. Upon being extracted from biological membranes and rendered water-soluble by their association with detergents, as is traditionally done, they tend to rapidly lose their functionality. As an alternative, MPs can be kept soluble in detergent-free solutions by trapping them with amphipathic polymers called amphipols (APols) (Tribet et al. 1996; Popot et al. 2011; Zoonens and Popot 2014). Due to a combination of factors, among which the low detergency of APols, their very low critical aggregation concentration, and their damping effect on MP dynamics (see Popot et al. 2011; Giusti et al. 2012; Perlmutter et al. 2014), most APol-trapped MPs are significantly more stable than their detergent-solubilized counterparts (reviewed in Popot 2010; Popot et al. 2003, 2011; Kleinschmidt and Popot 2014). APols do not desorb spontaneously from MPs even at extreme dilutions (Zoonens et al. 2007; Tribet et al. 2009), and fluorescence and surface plasmon resonance experiments show that APol-trapped MPs immobilized onto solid supports remain stable and functional even after extensive flushing with APol-free solutions (Charvolin et al. 2009). Under such conditions, it is possible to study MP/APol complexes without any interference by free APol.

These properties of APols point to their potential usefulness for performing MP SERS studies. It seems feasible indeed to insert MP/APol complexes, whose size is typically in the 5–10 nm range, in hot spots of appropriate SERS substrates, for example in the gaps between silver NPs, where Raman signals can become enhanced by factors between $\sim 10^7$ (5-nm gap) and $\sim 10^5$ (10-nm gap) (Xu et al. 1999, 2000, 2001). It has been suggested that SM sensitivity can be achieved provided the effective SERS cross section of a molecule is $\geq 10^{-19}$ cm^2 (Le Ru and Etchegoin 2012). An enhancement by 10^7 therefore in principle allows to detect a single MP with a Raman cross section $\geq 10^{-26}$ cm^2. Such values are observed at least under resonance Raman (RR)

conditions. For example, the Raman cross section of bacteriorhodopsin (BR), a light-driven proton pump from *Halobacterium salinarum*, is $\sim 10^{-24}$ to 10^{-23} cm^2 per molecule for some Raman bands of its chromophore, retinal, under resonance laser excitation at 514.5 nm (Myers et al. 1983). An enhancement by 10^4–10^5 should therefore suffice to observe SERS by a single-BR molecule. Thus, the use of APols for keeping soluble and stabilizing MPs could open the way to SM SERS studies of MPs, at least if one can combine RR and SERS. It should also be mentioned that coherent anti-Stokes Raman scattering (CARS) (Begley et al. 2003) in combination with SERS may be another way to obtain RS by SMs (Koo et al. 2005; Steuwe et al. 2011), because CARS spectroscopy provides enhancements of several orders of magnitude relative to conventional Raman spectroscopy.

BR is one of the best characterized MPs, which has been studied by a vast array of biophysical techniques (see e.g., Maeda 1995; Lanyi 2004; Hirai et al. 2009; Morgan et al. 2012), including Raman spectroscopy (Smith et al. 1985; Nabiev et al. 1990; Mathies 1991). Furthermore, BR has been used as a model MP to develop APols, and its complexes with the polyacrylate-based APol A8-35 (Tribet et al. 1996) have been extensively studied (Pocanschi et al. 2006; Gohon et al. 2008; Charvolin et al. 2009; Dahmane et al. 2013; Etzkorn et al. 2013, 2014; Elter et al. 2014). When BR is transferred to A8-35 from a solution of detergent-solubilized purple membrane, as has been done in the present work, the complexes comprise the protein, purple membrane lipids, and ~ 2 g of APol per g of protein (Gohon et al. 2008). APol-trapped BR is functional and highly stable (Gohon et al. 2008; Dahmane et al. 2013). It can be immobilized onto solid supports, using various tagged APols, and flushed with surfactant-free buffers without denaturation (Charvolin et al. 2009; Della Pia et al. 2014a, b; Le Bon et al. 2014). In the present study, BR/A8-35 complexes have been used to explore the feasibility of studying APol-trapped MPs by SERS. We found that A8-35-trapped BR stays native and stable even in a dried state at low humidity, which allows one to assemble it with noble metal NPs. A dried mixture of BR/A8-35 solution and Ag NPs colloid prepared by the Lee-Meisel method (Lee and Meisel 1982) showed considerable enhancement of Raman signals. The SERS spectrum of A8-35-trapped BR is similar to the non-SERS spectrum of the same complexes in the dried state at low humidity, with an average SERS enhancement by at least 10^2.

Materials and Methods

Chemicals

n-Octyl-β-D-glucopyranoside (OG), potassium dihydrogen phosphate (KH_2PO_4), disodium hydrogen phosphate (Na_2HPO_4), trisodium citrate dihydrate, and silver nitrate were purchased from Sigma Aldrich (France). Bio-Beads SM-2 adsorbent was obtained from Bio-Rad (France). Amphipol A8-35 was synthesized by F. Giusti (UMR 7099) as described in refs. (Gohon et al. 2004, 2006).

Purple Membrane Purification and BR Solubilization

Purple membranes were extracted from *Halobacterium salinarum* S9 (Oesterhelt and Stoeckenius 1974), and purified and solubilized in OG as described in detail in (Gordeliy et al. 2003; Borshchevskiy et al. 2011), except that 20 mM Na_2HPO_4/KH_2PO_4 (Na/K–P_i) buffer, pH 7.1, was used as a solubilization buffer instead of 20 mM Na/K–P_i buffer, pH 6.9.

The concentration of solubilized BR was estimated by UV–Visible (UV–Vis) absorption spectroscopy using $\varepsilon_{554} = 47$ mM^{-1} cm^{-1} and $\varepsilon_{280} = 81$ mM^{-1} cm^{-1} (Gohon et al. 2008; London and Khorana 1982) and was typically equal to 2.5 g L^{-1}.

Preparation of BR/A8-35 Complexes

The preparation of BR/A8-35 complexes was performed as described in ref. (Gohon et al. 2008). A8-35 from a 10 % w/w stock solution in water was added to BR solubilized in OG at 5:1 w/w APol/BR. After 15 min, detergent adsorption onto Bio-Beads SM-2 (10 g per g OG) was carried out for 2 h under gentle stirring and the Bio-Beads were removed. The concentration of BR was estimated by UV–Vis absorption and typically was equal to 2–2.5 g L^{-1}.

According to ref. (Gohon et al. 2008), the weight ratio of BR/A8-35 in the complexes is approximately equal to 1:2, whereas to prepare them A8-35 is added to OG-solubilized BR in a weight ratio of 5:1. The concentration of A8-35 can be estimated by Fourier transform infrared (FTIR) spectroscopy in the wavelength range from 400 to 3,000 cm^{-1}. To remove the excess of free, unbound A8-35, the following procedure was used. The BR/A8-35 solution was concentrated to 30 g L^{-1} by 15 min of centrifugation at 3,000×*g* in a 100-kDa cut-off centrifugal filter (Vivaspin 500, Vivasciences, USA), after which the FTIR absorption spectrum of the 30 g L^{-1} BR/A8-35 solution was measured with a FTIR spectrometer Vertex 70 (Bruker, Germany). After the FTIR measurement, the solution was diluted 5× with 20 mM Na/K–P_i buffer, pH 7.1, and again concentrated to 30 g L^{-1} by 10 min of centrifugation at 3,000×*g* in the 100-kDa cut-off centrifugal filter. This dilution–concentration step was repeated $\sim 4\times$ until there were no detectable changes in the FTIR spectrum of the concentrated solution, indicating that unbound APol molecules had been essentially eliminated from the solution. The solution at 30 g L^{-1} BR concentration was diluted

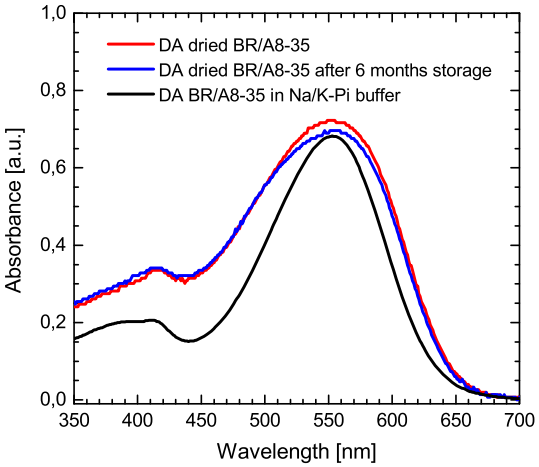

Fig. 1 UV-Visible absorption spectra of dark-adapted (DA) BR/A8-35 complexes in 20 mM Na/K–P_i pH 7.2 buffer (*black line*), of a DA dried BR/A8-35 film (*red line*), and of the same film after 6-month storage in the dark at 22 °C at ~50 % humidity (*blue line*) (Color figure online)

with 20 mM Na/K-P_i buffer, pH 7.1, 2 g L^{-1} BR concentration. The final solution was stored in the dark at 4 °C and used for further experiments.

Preparation of Ag NP Solution

The Ag NP colloid solution was prepared by the Lee–Meisel method (Lee and Meisel 1982). The basic procedure comprised the following steps: 90 mg of $AgNO_3$ was added into 500 mL of pure water and heated up to 100 °C. 10 mL of 1 % sodium citrate was added and the solution boiled for 1.5 h. The resulting silver colloid had a peak of UV–Visible absorption at 405 nm, with a full width at half height of ~102 nm (Fig. S1).

Preparation of Samples for UV–Visible Absorption and Raman Spectroscopy Experiments

In order to avoid the formation of salt crystals during drying, the concentration of Na/K–P_i buffer in the BR/A8-35 solution was reduced to the nM range by several dilution–concentration steps using a 100-kDa cut-off centrifugal filter, as described in the previous section, except that deionized water (Milli-Q, Millipore) was used for dilution instead of the 20 mM Na/K–P_i buffer. 4 µL of the resulting solution of "BR/A8-35 in water" (8 g L^{-1} BR) was deposited on a clean siliconized glass slide HR3-215 (Hampton Research, USA) and dried during 12 h in the dark at 22 °C under ~50 % humidity.

The UV–Visible absorption spectrum of the dried BR/A8-35 film was measured, in the dark-adapted state (Lanyi 2004), right after the drying process and was controlled during 6 months of storage in the dark at 22 °C under ~50 % humidity (Fig. 1).

For SERS measurements, 1 mL of Ag NP suspension was placed in an 1.5-mL Eppendorf tube and the NPs concentrated by centrifugation for 30 min at 3,000×*g*. 950 µL of supernatant was removed, after which 950 µL of the "BR/A8-35 in water" solution at 0.08 g L^{-1} BR was added to the concentrated Ag NP suspension (of 50-µL volume) and the NPs resuspended by vortexing. This centrifuging–resuspending step was repeated 7× to reduce the concentration of reactants remaining after the synthesis of Ag NPs (Munro et al. 1995) to the pM range, in order to avoid the detection of spurious SERS signals from the reactants. The resulting 1-mL mixture of BR/A8-35 complexes and Ag NPs was again centrifuged for 30 min at 3,000×*g*. 950 µL of supernatant was removed, and the NPs were redispersed in the remaining 50 µL by vortexing. 5 µL of the concentrated BR/A8-35–Ag NPs solution were deposited on a glass slide HR3-215 and dried during 12 h in the dark at 22 °C under ~50 % humidity. The resulting dried drop was used for SERS experiments.

To evaluate the SERS enhancement factor (EF), 5 µL of the "BR/APol A8-35 in water" solution at 0.8 g L^{-1} BR was deposited on a siliconized glass slide HR3-215, dried during 12 h in the dark at 22 °C under ~50 % humidity, and used for resonance Raman measurements.

UV–Visible Absorption Spectroscopy

All absorption spectra were measured with a UV2450 spectrophotometer (Shimadzu, Japan).

Raman Measurements

For Raman measurements, we used a microspectrophotometer based on a spectrograph Renishaw InVia (UK), which has been described in detail in ref. (Carpentier et al. 2007). All RS spectra were collected in backscattering geometry with a 50× objective (which provided a collection area with a diameter of ~20 µm) at a laser wavelength of 514.5 nm and an exposure time of 30 s. The SERS sample was examined at 10 µW laser power. Liquid and dried BR samples (without Ag NPs) were examined at 20 and 1 mW laser powers, respectively.

Results and Discussion

UV–Visible Absorption Spectrum and Resonance Raman Spectra of Dried A8-35-Trapped BR

The procedure used to prepare SERS-active samples is to mix solutions of Ag NPs and BR/A8-35 complexes, deposit a drop of the mixture on a glass substrate, and dry it at a

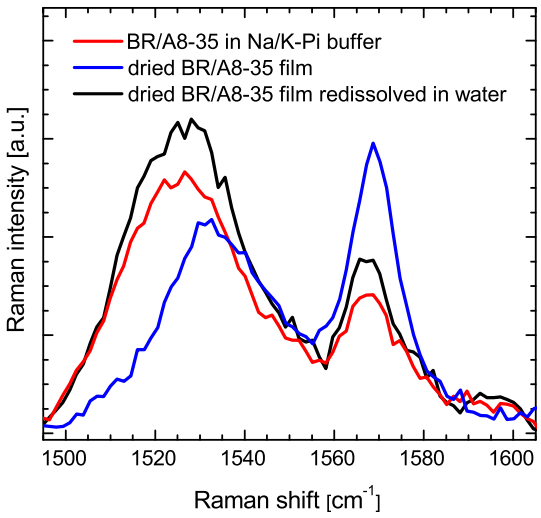

Fig. 2 Scaled resonance Raman spectra of BR/A8-35 complexes in 20 mM Na/K–P_i, pH 7.2 (*red line*), of a dried BR/A8-35 film (*blue line*), and of the same film after redissolution in water (*black line*) (Color figure online)

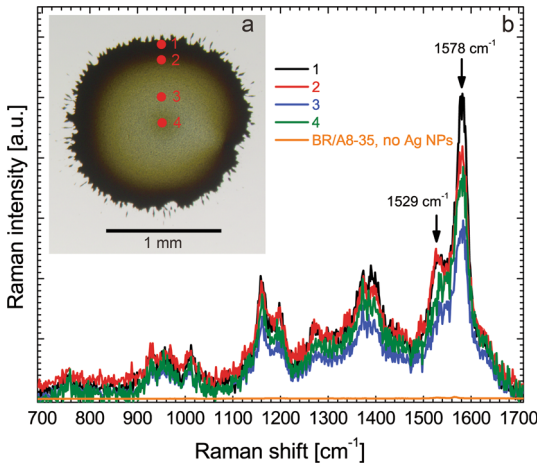

Fig. 3 **a** A bright-field optical image of a dried mixture of BR/A8-35 complexes and silver NPs (5-μL drop at a BR concentration of 0.08 g L^{-1}). **b** Four Raman spectra marked as *1* (*black line*), *2* (*red line*), *3* (*blue line*), and *4* (*green line*) are typical SERS spectra observed from the dried drop in **a**. These spectra were collected (30 s, 514.5-nm laser, 10-μW power) from the areas marked by red spots with corresponding numbers in **a**. The Raman spectrum drawn as an *orange line* is the RR spectrum collected (30 s, 514.5-nm laser, 1-mW power) from a dried 5-μL drop of A8-35-trapped BR (0.8 g L^{-1} BR) in the absence of NPs, normalized to the acquisition parameters of the SERS spectra, neglecting the higher concentration of BR in the RR sample (Color figure online)

relative humidity of ~50 %. A8-35-trapped BR remains properly folded after this procedure, as indicated by its native purple color and by the similarity of the UV–Visible absorption spectra of dark-adapted BR/A8-35 complexes in aqueous solution and in dried form, both of which present an absorption maximum at ~552 nm (Fig. 1). The complexes in the dried form are highly stable, almost no changes in their spectrum being observed after 6 months of storage of the dried films in the dark at 22 °C (Fig. 1).

RR spectra (Fig. 2) from both BR/A8-35 complexes in solution in Na/K–P_i buffer and the dried films feature peaks in the range 1,500–1,600 cm^{-1} (Smith et al. 1985; Diller and Stockburger 1988), revealing the presence of different retinal conformational states, spectrally assigned to the light-adapted and dark-adapted resting states of BR, characterized by the 1,526–1,536 cm^{-1} Raman lines (Smith et al. 1987a, b), and to the M-state of BR, an intermediate in the photocycle, characterized by the 1,566 cm^{-1} Raman line (Braiman and Mathies 1980; Smith et al. 1985). These peaks are usually assigned to C=C stretches of retinal (Smith et al. 1985; Diller and Stockburger 1988). Dried BR/A8-35 films redissolved in water and BR/A8-35 complexes kept in Na/K–P_i buffer exhibit similar RR spectra (Fig. 2), indicating that the different intensity ratios of the ~1,530 and 1,566 cm^{-1} lines are likely caused by drying and/or immobilization of BR/A8-35 complexes, rather than unfolding of BR molecules.

The RR peaks cannot be assigned to vibrations of A8-35 molecules. Indeed, Stokes Raman lines were not detected, in the range of 1,500–1,600 cm^{-1}, when a 100 g L^{-1} A8-35 solution was observed under the same Raman signal acquisition conditions as for the 2 g L^{-1} A8-35-trapped BR in solution, where the APol concentration cannot exceed ~10 g L^{-1}, given the procedure used for the preparation of BR/A8-35 complexes. This indicates that A8-35 molecules have a much lower Raman cross section than BR molecules in the range 1,500–1,600 cm^{-1} under 514.5-nm laser excitation. This silence of A8-35 makes it possible to detect even weak RR signals of BR.

All the aforementioned leads to the conclusion that, in a dried state, A8-35-trapped BR undergoes its photocycle after green (514.5 nm) laser excitation, but probably with intermediate states and relaxation times different from those of the solution form (Gohon et al. 2008), as observed in the case of the dried versus suspended forms of purple membranes (Korenstein and Hess 1977a, b; Lazarev and Evgeni 1980; Hildebrandt and Stockburger 1984; Váró and Lanyi 1991). Indeed, a longer life time of the M-state, as observed for partially dried purple membrane (Korenstein and Hess 1977b; Lazarev and Evgeni 1980), could account for the higher intensity of the 1,566-cm^{-1} peak relative to the 1,530-cm^{-1} one.

It is worth mentioning that A8-35-trapped BR in solution has nearly the same RR spectrum as BR in native purple membranes (Fig. S2), as expected given that it contains *all-trans* retinal in its ground state and has photochemistry kinetics similar to that in purple membranes (Gohon et al. 2008; Dahmane et al. 2013).

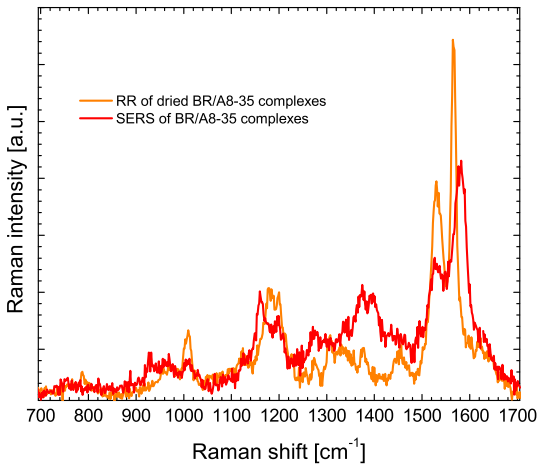

Fig. 4 SERS spectrum *2* (from Fig. 3) from a dried drop of BR/A8-35 complexes mixed with Ag NPs (*red line*) and scaled RR spectrum of dried BR/A8-35 complexes in the absence of NPs (*orange line*) (Color figure online)

SERS Spectrum of A8-35-Trapped BR

A microscopic image of a dried mixture of BR/A8-35 and Ag NPs is presented in Fig. 3a. The different colors are due to the non-uniform distribution and aggregation of Ag NPs, which usually occur during the drying process (Félidj et al. 1999; Wang et al. 2008; Avci and Culha 2013). The non-uniform aggregation of Ag NPs results in variable degrees of red shift and broadening of the plasmon peak (Félidj et al. 1999; Wang et al. 2008) and causes the UV–Visible absorption spectrum to vary along the dried drop (Fig. S1). Upon scanning the sample and accumulating Raman signals from various points of the sample, all SERS spectra were found to be qualitatively similar to each other, and SERS peaks were observed at identical positions with relative intensities (for example, for 1,529 and 1,578 cm^{-1} lines) varying by a factor <2 (Fig. 3b).

The SERS spectra qualitatively resemble the RR spectrum of BR/A8-35-dried films (Fig. 4; Table 1). Significant differences of peak positions and intensity ratios do exist, however. They may be caused by the influence of surface plasmon on retinal photochemistry (Biesso et al. 2008, 2009; Yen et al. 2010) and/or by the dependence of SERS electromagnetic enhancement on the distance between chemical bonds of the analyte and the metal surface (Kennedy et al. 1999; Dick et al. 2000; Stiles et al. 2008), which may vary depending on the local nanostructure of the NP/BR aggregates. It is known that the electromagnetic field of surface plasmons decays dramatically with the distance from the surface of a noble metal NP (Hao and Schatz 2003; Stiles et al. 2008). Nevertheless, the band around 1,530 cm^{-1} of C=C retinal stretches, a marker for BR in its light-adapted and dark-adapted states (Smith et al. 1985), is observed for both RR and SERS spectra of BR/A8-35.

Table 1 Raman bands detected from dried films of BR/A8-35 complexes with and without Ag NPs

SERS spectrum of BR/A8-35 (with Ag NPs) (cm^{-1})	RR spectrum of BR/A8-35 (without Ag NPs), (cm^{-1})
754 w	786 w
928 w	954 w
963 w	975 w
	985 w
1,009 w	1,010 m
1,029 w	
1,123 w	1,123 w
1,161 m	1,182 m
1,197 m	1,199 m
1,275 w	1,275 w
	1,306 w
1,343 w	
1,373 m	1,376 w
1,395 m	
	1,453 w
1,529 m	1,530 s
1,578 s	1,566 s
	1,620 w

Relative intensities are marked as w (weak), m (medium), s (strong)

The SERS spectra obtained from BR/A8-35 complexes qualitatively resemble tip-enhanced Raman scattering (TERS) and SERS spectra obtained from purple membranes (Deckert-Gaudig et al. 2012; Nabiev et al. 1985, 1990). TERS spectra of purple membranes (Deckert-Gaudig et al. 2012) also show point-to-point variations, a phenomenon attributed to the small number of molecules under the silver-coated AFM tip and differences in their orientation. The variability we observe from point to point suggests that SERS signals are dominated by the contributions of a limited number of BR molecules, which experience particularly high EFs.

The average SERS EF (Stiles et al. 2008) is equal to the ratio of SERS band intensities of an analyte molecule to the Raman line intensities, normalized to laser excitation power and analyte concentration. To evaluate the minimum SERS EF, we took the minimum intensity observed for the 1,529-cm^{-1} line from our SERS sample (5-μL drop of 0.08 g L^{-1} BR mixed with Ag NPs, 10 μW laser power, ~1.5-mm drop diameter) and the maximum intensity for the 1,530 cm^{-1} line observed from the dried BR/APol film (5-μL drop of 0.8-g L^{-1} BR without Ag NPs deposited on a glass slide, 1-mW laser power, ~2.6-mm dried drop diameter). Assuming for EF estimation uniform area

distribution of BR in the samples, the intensities were normalized to the BR concentrations (divided by the area of the dried drop) and to the 514.5-nm laser acquisition powers. The resulting minimum SERS EF was found to be $>10^2$.

Because of non-uniform sample and EF distribution in aggregated Ag NPs colloids of the SERS sample, which is mainly caused by "hot spot" formation in gaps between NPs (Corni and Tomasi 2002; Xu and Käll 2003; Le Ru et al. 2006a; Le Ru and Etchegoin 2012), it can be assumed that only a small percentage of BR molecules contributes to the overall SERS signal, and that the EFs for these molecules are much larger than 10^2, perhaps 10^5 or more if less than one molecule in 1,000 sits in a SERS-favorable position. Such a factor, as was mentioned above, could be enough to detect a Raman signal from a single BR molecule. Further experiments are obviously necessary to directly prove the experimental feasibility of performing SM SERS experiments with A8-35-trapped BR.

Apart from SM studies, SERS measurements on APol-trapped MPs can open the way to creating supersensitive sensors, which could allow one to observe conformation changes of MPs, e.g., upon ligand binding, or as a result of site-directed mutations, using very small amount of analyte relative to conventional Raman spectroscopy, as has been demonstrated for water-soluble proteins (e.g., Chumanov et al. 1990; Drachev et al. 2005; Siddhanta and Naray 2012). A particularly tantalizing suggestion would be to use the APol itself to bind MPs to SERS substrates, as has been done for surface plasmon resonance experiments (Charvolin et al. 2009; Della Pia et al. 2014a, b). In particular, one could make use, for this purpose, of a recently developed thiamorpholine-carrying variant of A8-35 ("SulfidAPol"; Zoonens and Popot 2014, and unpublished data). SulfidAPol could be used to bind MPs to the surface of gold or gold-coated silver colloidal or nanostructured SERS substrates, thereby placing a high proportion of APol-trapped MPs in hot spots, which could conceivably increase the average EF observed in the present work by several orders of magnitude (cf. Cui et al. 2006; Stiles et al. 2008; Yang et al. 2008; Coluccio et al. 2009; Patra and Kumar 2013).

It is fair to note that the variability of SERS spectra from one point to another of the samples (presumably due to the non-uniform distribution of local orientations of MP molecules relative to the surface of the SERS substrate, as mentioned above) complicates their analysis. Perhaps, the problem can be solved by averaging many SERS spectra, until no significant changes are observed anymore, or by creating SERS substrates that provide a more uniform (relative to the size of a Raman collection spot) EF distribution and analyte orientation.

Conclusions

The present data show that BR trapped in APol is highly stable even at low humidity, and suitable for SERS experiments. Ag NPs were mixed with A8-35-trapped BR, and the aggregates formed upon drying the mixture were found to be highly SERS-active. The estimated average SERS enhancement was estimated to be at least 10^2. According to the literature, the aggregation of noble metal NPs leads to formation of so-called "hot spots" in the gaps between NPs, where SERS enhancement can be much higher than 10^5, which is estimated to be suitable to perform SM SERS with BR. Besides SM SERS studies, it seems that APols can be potentially suitable for creating SERS sensors that could detect conformational changes of MPs using much lower amounts of protein than is required for conventional Raman spectroscopy.

Acknowledgments We are deeply thankful to Fabrice Giusti (UMR 7099) for synthesizing the amphipols used in the present work. The Raman scattering experiments and UV–Visible absorbance spectroscopy measurements were performed at the ID29S-Cryobench platform of the Grenoble Instruct centre (ISBG; UMS 3518 CNRS-CEA-UJF-EMBL) with support from the European Synchrotron Radiation Facility (ESRF), FRISBI (ANR-10-INSB-05-02) and GRAL (ANR-10-LABX-49-01) within the Grenoble Partnership for Structural Biology (PSB), located next to beamline ID29 of the ESRF. This work was supported by the program "Chaires d'excellence, édition 2008" of the Agence Nationale de la Recherche France, by the Commissariat à l'Énergie Atomique (Institut de Biologie Structurale), by the Helmholtz Gemeinschaft (Research Centre Jülich) Special Topic of Cooperation 5.1 specific agreement, by a Marie Curie grant (Seventh Framework Programme-PEOPLE-2007-1-1-Initial Training Networks, project Structural Biology of Membrane Proteins), by a European Commission Seventh Framework Programme grant for the European Drug Initiative on Channels and Transporters consortium (HEALTH-201924), by the Centre National pour la Recherche Scientifique, by University Paris 7, and by the "Initiative d'Excellence" program of the French State (Grant "DYNAMO," ANR-11-LABX-0011-01). Vitaly Polovinkin is very grateful to the Fondation Nanosciences for financial support. Part of this work was supported by the German Ministry of Education and Research (PhoNa-Photonic Nanomaterials). We acknowledge support of this work by the Russian Foundation for Basic Research (Research projects 13-04-91320 and 13-04-01700), by the Russian program "5Top100" and by the Ministry of Education and Science of the Russian Federation. This work was supported by ONEXIM, Russia.

References

Albrecht MG, Creighton JA (1977) Anomalously intense Raman spectra of pyridine at a silver electrode. J Am Chem Soc 99:5215–5217

Avci E, Culha M (2013) Influence of droplet drying configuration on surface-enhanced Raman scattering performance. RSC Adv 3:17829–17836

Begley RF, Harvey AB, Byer RL (2003) Coherent anti-Stokes Raman spectroscopy. Appl Phys Lett 25:387–390

Benevides JM, Overman SA, Thomas GJ (2004) Raman spectroscopy of proteins. In: Current protocols in protein science. John Wiley & Sons, Inc, US, pp 17.8.1-17.8.35

Biesso A, Qian W, El-Sayed MA (2008) Gold nanoparticle plasmonic field effect on the primary step of the other photosynthetic system in nature, bacteriorhodopsin. J Am Chem Soc 130:3258–3259

Biesso A, Qian W, Huang X, El-Sayed MA (2009) Gold nanoparticles surface plasmon field effects on the proton pump process of the bacteriorhodopsin photosynthesis. J Am Chem Soc 131:2442–2443

Borshchevskiy VI, Round ES, Popov AN, Büldt G, Gordeliy VI (2011) X-ray-radiation-induced changes in bacteriorhodopsin structure. J Mol Biol 409:813–825

Braiman M, Mathies R (1980) Resonance Raman evidence for an *all-trans* to 13-*cis* isomerization in the proton-pumping cycle of bacteriorhodopsin. Biochemistry 19:5421–5428

Carey P (1982) Biochemical applications of Raman and resonance Raman spectroscopies. Elsevier, New York

Carpentier P, Royant A, Ohana J, Bourgeois D (2007) Advances in spectroscopic methods for biological crystals. 2. Raman spectroscopy. J Appl Crystallogr 40:1113–1122

Charvolin D, Perez J-B, Rouvière F, Giusti F, Bazzacco P, Abdine A, Rappaport F, Martinez KL, Popot J-L (2009) The use of amphipols as universal molecular adapters to immobilize membrane proteins onto solid supports. Proc Natl Acad Sci USA 106:405–410

Chumanov GD, Efremov RG, Nabiev IR (1990) Surface-enhanced Raman spectroscopy of biomolecules. Part I.—Water-soluble proteins, dipeptides and amino acids. J Raman Spectrosc 21:43–48

Coluccio ML, Das G, Mecarini F, Gentile F, Pujia A, Bava L, Tallerico R, Candeloro P, Liberale C, De Angelis F, Di Fabrizio E (2009) Silver-based surface enhanced Raman scattering (SERS) substrate fabrication using nanolithography and site selective electroless deposition. Microelectron Eng 86:1085–1088

Corni S, Tomasi J (2002) Surface enhanced Raman scattering from a single molecule adsorbed on a metal particle aggregate: a theoretical study. J Chem Phys 116:1156–1164

Cui Y, Ren B, Yao J-L, Gu R-A, Tian Z-Q (2006) Synthesis of $Ag_{core}Au_{shell}$ bimetallic nanoparticles for immunoassay based on surface-enhanced Raman spectroscopy. J Phys Chem B 110:4002–4006

Dahmane T, Rappaport F, Popot J-L (2013) Amphipol-assisted folding of bacteriorhodopsin in the presence or absence of lipids: functional consequences. Eur Biophys J 42:85–101

Deckert-Gaudig T, Böhme R, Freier E, Sebesta A, Merkendorf T, Popp J, Gerwert K, Deckert V (2012) Nanoscale distinction of membrane patches—a TERS study of *Halobacterium salinarum*. J Biophotonics 5:582–591

Delfino I, Bizzarri AR, Cannistraro S (2006) Time-dependent study of single-molecule SERS signal from yeast cytochrome *c*. Chem Phys 326:356–362

Della Pia EA, Holm JV, Lloret N, Le Bon C, Popot J-L, Zoonens M, Nygård J, Martinez KL (2014a) A step closer to membrane protein multiplexed nanoarrays using biotin-doped polypyrrole. ACS Nano 8(2):1844–1853

Della Pia EA, Westh Hansen R, Zoonens M, Martinez KL (2014b) Functionalized amphipols: a versatile toolbox suitable for applications of membrane proteins in synthetic biology. J Membr Biol. doi:10.1007/s00232-014-9663-y

Dick LA, Haes AJ, Van Duyne RP (2000) Distance and orientation dependence of heterogeneous electron transfer: a surface-enhanced resonance Raman scattering study of cytochrome *c* bound to carboxylic acid terminated alkanethiols adsorbed on silver electrodes. J Phys Chem B 104:11752–11762

Diller R, Stockburger M (1988) Kinetic resonance Raman studies reveal different conformational states of bacteriorhodopsin. Biochemistry 27:7641–7651

Drachev VP, Thoreson MD, Khaliullin EN, Davisson VJ, Shalaev VM (2004) Surface-enhanced Raman difference between human insulin and insulin lispro detected with adaptive nanostructures. J Phys Chem B 108:18046–18052

Drachev VP, Thoreson MD, Nashine V, Khaliullin EN, Ben-Amotz D, Davisson VJ, Shalaev VM (2005) Adaptive silver films for surface-enhanced Raman spectroscopy of biomolecules. J Raman Spectrosc 36:648–656

Elter S, Raschle T, Arens S, Gelev V, Etzkorn M, Wagner G (2014) The use of amphipols for NMR structural characterization of 7-TM proteins. J Membr Biol. doi:10.1007/s00232-014-9669-5

Etzkorn M, Raschle T, Hagn F, Gelev V, Rice AJ, Walz T, Wagner G (2013) Cell-free expressed bacteriorhodopsin in different soluble membrane mimetics: biophysical properties and NMR accessibility. Struct Lond Engl 1993 21:394–401

Etzkorn M, Zoonens M, Catoire LJ, Popot J-L, Hiller S (2014) How amphipols embed membrane proteins: global solvent accessibility and interaction with a flexible protein terminus. J Membr Biol. doi:10.1007/s00232-014-9657-9

Félidj N, Aubard J, Lévi G (1999) Discrete dipole approximation for ultraviolet–visible extinction spectra simulation of silver and gold colloids. J Chem Phys 111:1195–1208

Fleischmann M, Hendra PJ, McQuillan AJ (1974) Raman spectra of pyridine adsorbed at a silver electrode. Chem Phys Lett 26:163–166

Futamata M (2006) Single molecule sensitivity in SERS: importance of junction of adjacent Ag nanoparticles. Faraday Discuss 132:45–61

Futamata M, Maruyama Y, Ishikawa M (2005) Critical importance of the junction in touching Ag particles for single molecule sensitivity in SERS. J Mol Struct 735–736:75–84

Giusti F, Popot J-L, Tribet C (2012) Well-defined critical association concentration and rapid adsorption at the air/water interface of a short amphiphilic polymer, amphipol A8-35: a study by Förster resonance energy transfer and dynamic surface tension measurements. Langmuir 28:10372–10380

Gohon Y, Pavlov G, Timmins P, Tribet C, Popot J-L, Ebel C (2004) Partial specific volume and solvent interactions of amphipol A8-35. Anal Biochem 334:318–334

Gohon Y, Giusti F, Prata C, Charvolin D, Timmins P, Ebel C, Tribet C, Popot J-L (2006) Well-defined nanoparticles formed by hydrophobic assembly of a short and polydisperse random terpolymer, amphipol A8-35. Langmuir 22:1281–1290

Gohon Y, Dahmane T, Ruigrok RWH, Schuck P, Charvolin D, Rappaport F, Timmins P, Engelman DM, Tribet C, Popot J-L, Ebel C (2008) Bacteriorhodopsin/amphipol complexes: structural and functional properties. Biophys J 94:3523–3537

Gordeliy VI, Schlesinger R, Efremov R, Büldt G, Heberle J (2003) Crystallization in lipidic cubic phases: a case study with bacteriorhodopsin. Methods Mol Biol Clifton NJ 228:305–316

Habuchi S, Cotlet M, Gronheid R, Dirix G, Michiels J, Vanderleyden J, De Schryver FC, Hofkens J (2003) Single-molecule surface enhanced resonance Raman spectroscopy of the enhanced Green Fluorescent Protein. J Am Chem Soc 125:8446–8447

Hao E, Schatz GC (2003) Electromagnetic fields around silver nanoparticles and dimers. J Chem Phys 120:357–366

Hildebrandt P, Stockburger M (1984) Role of water in bacteriorhodopsin's chromophore: resonance Raman study. Biochemistry 23:5539–5548

Hirai T, Subramaniam S, Lanyi JK (2009) Structural snapshots of conformational changes in a seven-helix membrane protein: lessons from bacteriorhodopsin. Curr Opin Struct Biol 19:433–439

Hrabakova J, Ataka K, Heberle J, Hildebrandt P, Murgida DH (2006) Long distance electron transfer in cytochrome *c* oxidase immobilised on electrodes. A surface enhanced resonance Raman spectroscopic study. Phys Chem Chem Phys 8:759–766

Jeanmaire DL, Van Duyne RP (1977) Surface Raman spectroelectrochemistry: Part I. Heterocyclic, aromatic, and aliphatic amines adsorbed on the anodized silver electrode. J Electroanal Chem Interfacial Electrochem 84:1–20

Jiang, Bosnick K, Maillard M, Brus L (2003) Single-molecule Raman spectroscopy at the junctions of large Ag nanocrystals. J Phys Chem B 107:9964–9972

Kennedy BJ, Spaeth S, Dickey M, Carron KT (1999) Determination of the distance dependence and experimental effects for modified SERS substrates based on self-assembled monolayers formed using alkanethiols. J Phys Chem B 103:3640–3646

Kleinschmidt JH, Popot J-L (2014) Folding and stability of integral membrane proteins in amphipols. Arch Biochem Biophys (in press)

Kneipp K, Wang Y, Kneipp H, Perelman LT, Itzkan I, Dasari RR, Feld MS (1997) Single molecule detection using surface-enhanced Raman scattering (SERS). Phys Rev Lett 78:1667–1670

Kneipp K, Kneipp H, Bohr HG (2006) Single-molecule SERS spectroscopy. In: Kneipp K, Moskovits M, Kneipp H (eds) Surface-enhanced Raman scattering. Springer, Berlin Heidelberg, pp 261–277

Koo T-W, Chan S, Berlin AA (2005) Single-molecule detection of biomolecules by surface-enhanced coherent anti-stokes Raman scattering. Opt Lett 30:1024–1026

Korenstein R, Hess B (1977a) Hydration effects on *cis–trans* isomerization of bacteriorhodopsin. FEBS Lett 82:7–11

Korenstein R, Hess B (1977b) Hydration effects on the photocycle of bacteriorhodopsin in thin layers of purple membrane. Nature 270:184–186

Krogh A, Larsson B, von Heijne G, Sonnhammer EL (2001) Predicting transmembrane protein topology with a hidden Markov model: application to complete genomes. J Mol Biol 305:567–580

Lanyi JK (2004) Bacteriorhodopsin. Annu Rev Physiol 66:665–688

Lazarev YA, Evgeni LT (1980) Effect of water on the structure of bacteriorhodopsin and photochemical processes in purple membranes. Biochim Biophys Acta 590:324–338

Le Bon C, Della Pia EA, Giusti F, Lloret N, Zoonens M, Martinez KL, Popot J-L (2014) Synthesis of an oligonucleotide-derivatized amphipol and its use to trap and immobilize membrane proteins. Nucleic Acids Res. doi:10.1093/nar/gku250

Le Ru EC, Etchegoin PG (2012) Single-molecule surface-enhanced Raman spectroscopy. Annu Rev Phys Chem 63:65–87

Le Ru EC, Etchegoin PG, Meyer M (2006a) Enhancement factor distribution around a single surface-enhanced Raman scattering hot spot and its relation to single molecule detection. J Chem Phys 125:204701

Le Ru EC, Meyer M, Etchegoin PG (2006b) Proof of single-molecule sensitivity in surface enhanced-Raman scattering (SERS) by means of a two-analyte technique. J Phys Chem B 110:1944–1948

Lee PC, Meisel D (1982) Adsorption and surface-enhanced Raman of dyes on silver and gold sols. J Phys Chem 86:3391–3395

London E, Khorana HG (1982) Denaturation and renaturation of bacteriorhodopsin in detergents and lipid-detergent mixtures. J Biol Chem 257:7003–7011

Maeda A (1995) Application of FTIR spectroscopy to the structural study on the function of bacteriorhodopsin. Isr J Chem 35:387–400

Mathies RA (1991) From femtoseconds to biology: mechanism of bacteriorhodopsin's light-driven proton pump. Proc Indian Acad Sci 103:283–293

Morgan JE, Vakkasoglu AS, Lanyi JK, Lugtenburg J, Gennis RB, Maeda A (2012) Structure changes upon deprotonation of the proton release group in the bacteriorhodopsin photocycle. Biophys J 103:444–452

Moskovits M (1985) Surface-enhanced spectroscopy. Rev Mod Phys 57:783–826

Munro CH, Smith WE, Garner M, Clarkson J, White PC (1995) Characterization of the surface of a citrate-reduced colloid optimized for use as a substrate for surface-enhanced resonance Raman scattering. Langmuir 11:3712–3720

Myers AB, Harris RA, Mathies RA (1983) Resonance Raman excitation profiles of bacteriorhodopsin. J Chem Phys 79:603–613

Nabiev IR, Efremóv RG, Chumanov GD (1985) The chromophore-binding site of bacteriorhodopsin. Resonance Raman and surface-enhanced resonance Raman spectroscopy and quantum chemical study. J Biosci 8:363–374

Nabiev IR, Chumanov GD, Efremov RG (1990) Surface-enhanced Raman spectroscopy of biomolecules. Part II. Application of short- and long-range components of SERS to the study of the structure and function of membrane proteins. J Raman Spectrosc 21:49–53

Naumann H, Klare JP, Engelhard M, Hildebrandt P, Murgida DH (2006) Time-resolved methods in Biophysics. 1. A novel pump and probe surface-enhanced resonance Raman approach for studying biological photoreceptors. Photochem Photobiol Sci 5:1103–1108

Nie S, Emory SR (1997) Probing single molecules and single nanoparticles by surface-enhanced Raman scattering. Science 275:1102–1106

Oesterhelt D, Stoeckenius W (1974) Isolation of the cell membrane of *Halobacterium halobium* and its fractionation into red and purple membrane. Methods Enzymol 31:667–678

Otto A (1984) Surface-enhanced Raman scattering: "Classical" and "Chemical" origins. In: Cardona PDM, Güntherodt PDG (eds) Light Scattering in solids IV. Springer, Berlin Heidelberg, pp 289–418

Overington JP, Al-Lazikani B, Hopkins AL (2006) How many drug targets are there? Nat Rev Drug Discov 5:993–996

Patra PP, Kumar GVP (2013) Single-molecule surface-enhanced Raman scattering sensitivity of Ag-core Au-shell nanoparticles: revealed by bi-analyte method. J Phys Chem Lett 4:1167–1171

Perlmutter JD, Popot J-L, Sachs JN (2014) Molecular dynamics simulations of a membrane protein/amphipol complex. J Membr Biol. doi:10.1007/s00232-014-9690-8

Peticolas WL (1995) Raman spectroscopy of DNA and proteins. In: Sauer K (ed) Methods in enzymology. Academic Press, London, pp 389–416

Pocanschi CL, Dahmane T, Gohon Y, Rappaport F, Apell H-J, Kleinschmidt JH, Popot J-L (2006) Amphipathic polymers: tools to fold integral membrane proteins to their active form. Biochemistry 45:13954–13961

Popot J-L (2010) Amphipols, nanodiscs, and fluorinated surfactants: three nonconventional approaches to studying membrane proteins in aqueous solutions. Annu Rev Biochem 79:737–775

Popot J-L, Berry EA, Charvolin D, Creuzenet C, Ebel C, Engelman DM, Flötenmeyer M, Giusti F, Gohon Y, Hong Q, Lakey JH, Leonard K, Shuman HA, Timmins P, Warschawski DE, Zito F, Zoonens M, Pucci B, Tribet C (2003) Amphipols: polymeric surfactants for membrane biology research. Cell Mol Life Sci 60:1559–1574

Popot J-L, Althoff T, Bagnard D, Banères J-L, Bazzacco P, Billon-Denis E, Catoire LJ, Champeil P, Charvolin D, Cocco MJ, Crémel G, Dahmane T, de la Maza LM, Ebel C, Gabel F, Giusti F, Gohon Y, Goormaghtigh E, Guittet E, Kleinschmidt JH, Kühlbrandt W, Le Bon C, Martinez KL, Picard M, Pucci B,

Sachs JN, Tribet C, van Heijenoort C, Wien F, Zito F, Zoonens M (2011) Amphipols from A to Z. Annu Rev Biophys 40:379–408

Siddhanta S, Naray C (2012) Surface-enhanced Raman spectroscopy of proteins: implications in drug designing. Nanomater Nanotechnol 2:1

Smith SO, Lugtenburg J, Mathies RA (1985) Determination of retinal chromophore structure in bacteriorhodopsin with resonance Raman spectroscopy. J Membr Biol 85:95–109

Smith SO, Pardoen JA, Lugtenburg J, Mathies RA (1987a) Vibrational analysis of the 13-*cis*-retinal chromophore in dark-adapted bacteriorhodopsin. J Phys Chem 91:804–819

Smith SO, Braiman MS, Myers AB, Pardoen JA, Courtin JML, Winkel C, Lugtenburg J, Mathies RA (1987b) Vibrational analysis of the all-*trans*-retinal chromophore in light-adapted bacteriorhodopsin. J Am Chem Soc 109:3108–3125

Steuwe C, Kaminski CF, Baumberg JJ, Mahajan S (2011) Surface enhanced coherent anti-Stokes Raman scattering on nanostructured gold surfaces. Nano Lett 11:5339–5343

Stiles PL, Dieringer JA, Shah NC, Van Duyne RP (2008) Surface-enhanced Raman spectroscopy. Annu Rev Anal Chem 1:601–626

Tribet C, Audebert R, Popot J-L (1996) Amphipols: polymers that keep membrane proteins soluble in aqueous solutions. Proc Natl Acad Sci 93:15047–15050

Tribet C, Diab C, Dahmane T, Zoonens M, Popot J-L, Winnik FM (2009) Thermodynamic characterization of the exchange of detergents and amphipols at the surfaces of integral membrane proteins. Langmuir 25:12623–12634

Váró G, Lanyi JK (1991) Thermodynamics and energy coupling in the bacteriorhodopsin photocycle. Biochemistry 30:5016–5022

Wang ZB, Luk'yanchuk BS, Guo W, Edwardson SP, Whitehead DJ, Li L, Liu Z, Watkins KG (2008) The influences of particle number on hot spots in strongly coupled metal nanoparticles chain. J Chem Phys 128:094705

Xu H, Käll M (2003) Polarization-dependent surface-enhanced Raman spectroscopy of isolated silver nanoaggregates. ChemPhysChem 4:1001–1005

Xu H, Bjerneld EJ, Käll M, Börjesson L (1999) Spectroscopy of single hemoglobin molecules by surface enhanced Raman scattering. Phys Rev Lett 83:4357–4360

Xu H, Aizpurua J, Käll M, Apell P (2000) Electromagnetic contributions to single-molecule sensitivity in surface-enhanced Raman scattering. Phys Rev E 62:4318–4324

Xu H, Bjerneld EJ, Aizpurua J, Apell P, Gunnarsson L, Petronis S, Kasemo B, Larsson C, Hook F, Kall M (2001) Interparticle coupling effects in surface-enhanced Raman scattering. In: BiOS 2001, the international symposium on biomedical optics. International Society for Optics and Photonics, pp 35–42

Yang Y, Shi J, Kawamura G, Nogami M (2008) Preparation of Au–Ag, Ag–Au core–shell bimetallic nanoparticles for surface-enhanced Raman scattering. Scr Mater 58:862–865

Yen C-W, Chu L-K, El-Sayed MA (2010) Plasmonic field enhancement of the bacteriorhodopsin photocurrent during its proton pump photocycle. J Am Chem Soc 132:7250–7251

Zoonens M, Popot J-L (2014) Amphipols for each season. J Membr Biol. doi:10.1007/s00232-014-9666-8

Zoonens M, Giusti F, Zito F, Popot J-L (2007) Dynamics of membrane protein/amphipol association studied by Förster resonance energy transfer: implications for in vitro studies of amphipol-stabilized membrane proteins. Biochemistry 46: 10392–10404